ISBN : **979-587-705-4**
*Vol. **3** No. **1***

Trabecular Bone Segmentation Based on Segment Profile Characteristics Using Extreme Learning Machine on Dental Panoramic Radiographs

Rizqi Okta Ekoputris
Department of Informatics
Institut Teknologi Sepuluh Nopember (ITS)
Surabaya, Indonesia
rizqi.okta@gmail.com

Arya Yudhi Wijaya
Department of Informatics
Institut Teknologi Sepuluh Nopember (ITS)
Surabaya, Indonesia
arya@if.its.ac.id

Agus Zainal Arifin
Department of Informatics
Institut Teknologi Sepuluh Nopember (ITS)
Surabaya, Indonesia
agusza@cs.its.ac.id

Dini Adni Navastara
Department of Informatics
Institut Teknologi Sepuluh Nopember (ITS)
Surabaya, Indonesia
dini_navastara@if.its.ac.id

Abstract*— Dental panoramic radiograph contains a lot of Information which one of them can be identified from trabecular bone structure. This research proposes segmentation of trabecular bone area on dental panoramic radiograph based on segment profile characteristics using Extreme Learning Machine as classification method. The input of this method is dental panoramic radiograph. The selection of region of interest (ROI) is performed on the lower jawbone of the trabecular bone area in which there are teeth and cortical bone. The ROI is subdivided into two where the upper ROI contains the teeth and the lower ROI contains cortical bone. After that, the result of the ROI deduction is done by preprocessing using mean and median filters for upper ROI and motion blur filter for lower ROI. The separate images are extracted each pixel into four features consisting of image intensity, 2D Gaussian filter with two different sigma, and Log Gabor filter for upper ROI. For lower ROI, five feature extractions are image intensity, Gaussian 2D filter with [illegible] Gaussian. Then used some sample pixels as training data to create Extreme Learning Machine model. The output of this classifier is the segmentation area of trabecular bone. On the upper ROI, the average of sensitivity, specificity, and accuracy were 82.31%, 93.67%, and 90.33%, respectively. While on the lower ROI obtained the average of sensitivity, specificity, and accuracy of 95.01%, 96.50%, and 95.29%, respectively.

Keywords*— *dental panoramic radiograph, Extreme Learning Machine, Trabecular bone, segmentation.

I. INTRODUCTION

Dental panoramic radiograph is a two-dimensional x-ray image (2-D) of the teeth that records the entire mouth, including the teeth, the upper jaw, the lower jaw, the tissues and structures that surround it in a single image. Dental panoramic radiograph is an easy and inexpensive to be obtained so it is often used as a diagnostic tool for serious diseases such as osteoporosis [1]. In dental panoramic radiograph recorded various information that can be used as an indicator in identifying various diseases such as trabecular bone structure. However, in dental panoramic radiographs, trabecular bone is difficult to observe due to poor image quality, low image contrast, uneven illumination and high noise.

Previous research that used dental panoramic radiographs to detect trabecular bone was done by [illegible] scale line operator. Dewi. [3] Conducted research to detect trabecular bone areas using multi-scale linear operators and clustering to differentiate teeth and trabecular bone. Another study that utilized dental panoramic radiographs to detect trabecular bone was performed by Yuniarti [4]. This research uses textural information using statistical measurement that is first and second order measure. This study was conducted on lower mandibular ROI to differentiate the trabecular bone and cortical bone regions.

ELM is a feed forward artificial neural network (ANN) with only one hidden layer or more commonly

ISBN : 979-587-705-4
Vol. 3 No. 1

known as single hidden layer feed-forward neural network (SLFNs). ELM method has advantages in the complexity of learning because this method only do one time training weight process. Research conducted by Zhu et al. [5] using ELM proves that ELM has faster training time and segmentation time than SVM, Random Forest, and AdaBoost in retinal vein segmentation.

This research proposed segmentation of trabecular bone area on dental panoramic radiograph based on segment profile characteristics and classification method of Extreme Learning Machine (ELM). The segment characteristic profile of this image is selected to perform feature extraction in the segmentation process. The characteristic profile in question is to take the value of the intensity generated by various filters.

II. METHODOLOGY

The research focused on trabecular bone segmentation on dental panoramic radiographs. This research can be used to support the utilization of dental panoramic radiograph image in health field. The data used is dental panoramic radiograph image data. The output data of the application is a black and white image. The output data will be used as input data in the next process. To perform segmentation of trabecular bone area on dental panoramic radiograph image there are several steps that need to be done, namely preprocessing, feature extraction, segmentation, and post-processing as shown in Fig. 1.

A. ROI Selection

The selection of ROI in this research is done twice on each image with the size 256 × 128 on the left and right as shown in Fig. 2. Each selected ROI contains teeth and cortical bone. Then the ROI is subdivided into two regions at the top and bottom with size of 128 × 128. The ROI selected on this dental panoramic radiograph has a contrast difference in the upper ROI, which contains the trabecular bone, cortical bone area and the area below the jaw. Contrast differences are seen between the cortical bone and trabecular bone areas. This results in segmentation performed directly on upper ROI and lower ROI gives less accurate results. Therefore, ROI separation is required to be the upper ROI and lower ROI.

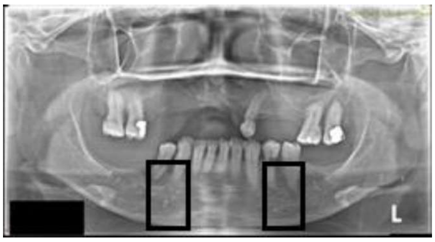

Fig. 1. ROI position of trabecular bone on dental panoramic radiograph

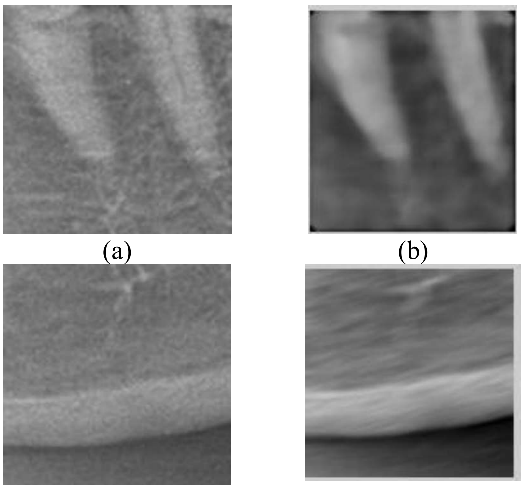

Fig. 2. ROI Image (a) upper ROI (b) result of preprocessing in upper ROI (c) lower ROI (d) result of preprocessing in lower ROI

Details of trabecular bone structures across the trabecular bone area may result in disruption of the segmentation process because the intensity of the pixels in the trabecular bone structure has a color like a tooth structure or cortical bone. If not refined or removed, this results in the segmentation process considering the trabecular bone structure as cortical bone or teeth. It is necessary to remove the trabecular bone structure.

B. Preprocessing

Preprocessing is a key step to do. In this research, the preprocessing step is image normalization, mean filter, median filter, and motion blur filter. Image normalization is done with
aim to equate the gray range between one image with another image. Mean filters and median filters are

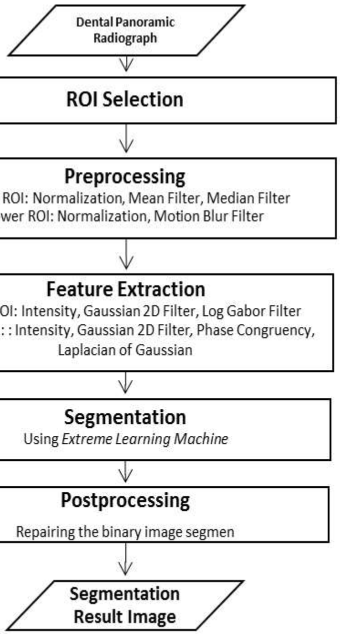

Fig. 3. Flowchart of segmenting trabecular bone area

used to remove noise in tooth image. In the upper ROI, a mean and median filter is performed after normalization. This is done because the noise is not irregular. But on the bottom ROI, used motion blur filter. This is because the noise on this ROI tend to be in the direction of cortical bone. With this motion blur filter, the noise will disappear but still strengthen the

ISBN : **979-587-705-4**
*Vol. **3** No. **1***

boundaries of each segment, especially the cortical bone that separates the trabecular bone from the background. The preprocessing results of upper and lower ROI are presented in Fig. 3.

C. Feature Extraction

The feature extraction process is performed to get the feature vector used in the segmentation classification process. In this research, the used feature extraction method are gaussian 2D filter, Log-Gabor filter, phase congruency, and Laplacian of Gaussian. The results of feature extraction are shown in Fig. 4 for upper ROI and Fig. 5 for lower ROI.

1) Gaussian 2D Filter

This filter is used to clarify the region of each segment. Gaussian filter is a filter that uses Gaussian function. Gaussian filtering is obtained from convolution operation. The multiplication operation performed is the multiplication of the kernel matrix with the original image matrix. The gaussian kernel matrix is derived from the computational function of the Gaussian distribution [6]. The first step is to read the image that has been in preprocessing. The second step is to build 2D Gaussian kernel. The third step is to convolution using the 2D Gaussian kernel. The sigma parameters used in this research are $\sqrt{2}$ and 2.

2) Log Gabor Filter

An alternative to the Gabor function is the Log-Gabor function proposed by Field (1987) [7]. Log-Gabor filters can be built with variable bandwidth and bandwidth can be optimized to produce filters with spatial boundaries. Fields indicate that the original image is better encoded with a filter that has a Gaussian transfer function when viewed from the logarithmic frequency scale. The Gabor function has a Gaussian transfer function when viewed from a linear frequency scale. Filters built on Log-Gabor use two components: the radial component, which controls the frequency band on the filter response and the angular component, which controls the orientation of the filter response.

The process of extracting Gabor Log filter feature is used to enhance the segments in the Fourier transform. This feature extraction is only used for upper ROI. The Gabor Log filter used in this method is Radial Log Gabor. The first step is to read the pre-processing image. The second step builds Radial Log Gabor kernel and transforms Fourier ROI image. The third step is to get an image that has been built with Radial Log Gabor filter. The parameters used are wavelength of 10 and sigma equal to 10.

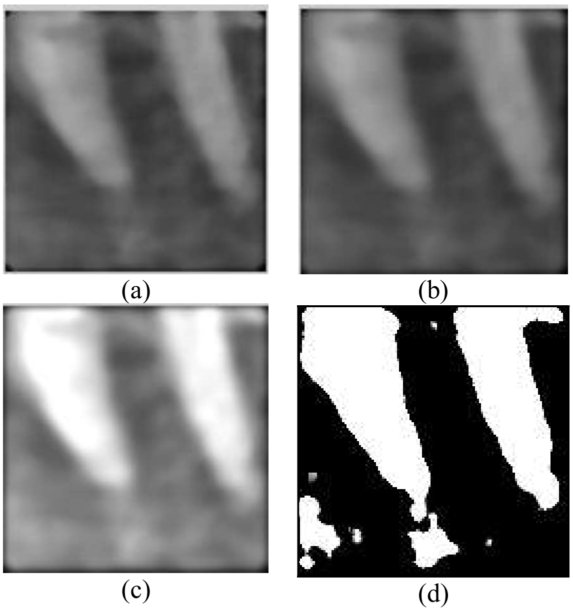

Fig. 5. Result of upper ROI filter (a) image preprocessing result (b) result of filter Gaussian 2D image using sigma = $\sqrt{2}$ (c) result of filter Gaussian 2D image using sigma = 2 (d) result of Log Gabor Filter

3) Phase congruency

Phase congruency demonstrates contrasting changes and invariant image brightness. Phase Congruency reflects image behavior in the frequency domain. It has been noted that the edge feature has

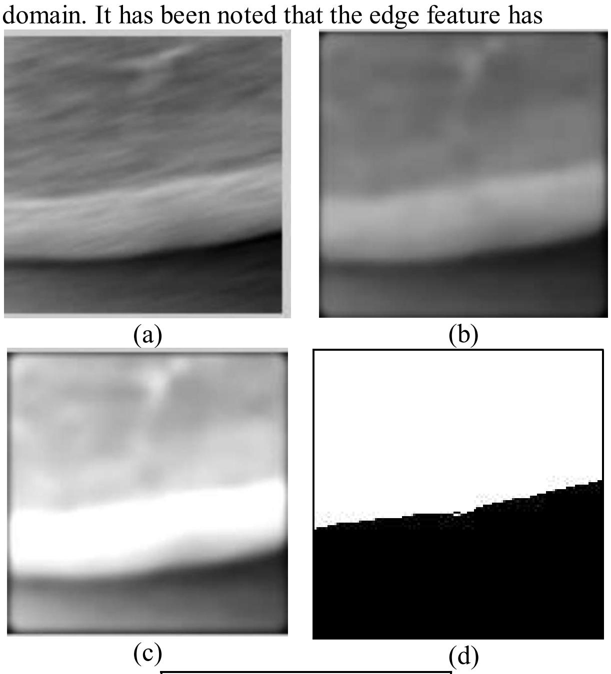

Fig. 4. Result of lower ROI filter (a) image preprocessing result (b) result of filter Gaussian 2D image using sigma = $\sqrt{2}$ (c) result of filter Gaussian 2D image using sigma = 2 (d) result of Phase Congruency (e) result of Laplacian of Gaussian

(e)

ISBN : 979-587-705-4
Vol. 3 No. 1

many frequency components in the same phase. This concept is similar to coherence, except that it applies to different wavelength functions. To compute all measurements in phase congruency on an image, an efficient model is proposed by Kovesi [8] in (1) where (x, y) is the position of the pixels. $A_{k,\theta}$ is a filtered image using the Log Gabor filter. k is a scale and θ is the six directions from 0 to π. $\lfloor\ \rfloor$ shows that the closest value equals its own value when it is positive, and zero for other than positive numbers. ε is a constant of small value and is used to prevent the zero distribution where the local energy is very small on the network image.

$$PC(x,y) = \frac{\sum_\theta \sum_k W_\theta(x,y) \lfloor A_{k,\theta} \Delta\Phi_{k,\theta}(x,y) - T_\theta \rfloor}{\sum_\theta \sum_k A_{k,\theta}(x,y) + \varepsilon} \qquad (1)$$

T_θ is the noise response used to reduce noise on energy calculations. W_θ is the weight factor that devalues phase congruency at the location where the filter spread is very thin. W_θ is obtained by the sigmoid function.

In this research, phase congruency filter is used to provide boundaries between segments especially the boundary between trabecular bone and cortical bone. This filter is only used for bottom ROI. Then we select the trabecular bone segment that is the uppermost segment. The first step is to read the bottom ROI image that has been preprocessing. Then in the second step is to design Angular Log Gabor filter at each orientation and transform the ROI image to Fourier form. The third step is to get an image that has been built using Angular Log Gabor filter. Then the fourth step is to get the sum of amplitude, even filter, and odd filter at each orientation. The fifth step is to calculate the phase congruency value of each pixel. Then the result of phase congruency is then binarized with parameter 0.3. The seventh step is to get the top edge cortical bone. The next step is to fill the segment above the edge.

4) Laplacian of Gaussian

Laplacian is a derived filter whose function can detect areas that have rapid changes like edges on an image. However, this laplacian is very vulnerable or sensitive to the presence of noise. To that end, the image to be detected by the flame is smoothed first by using Gaussian. Thus, it is known that the new derivative function is LoG or Laplacian of Gaussian. LoG formula as described in (2).

$$L(x,y) = \nabla^2 f(x,y) = \frac{\partial^2 f(x,y)}{\partial x^2} + \frac{\partial^2 f(x,y)}{\partial y^2} \qquad (2)$$

Then, combining the Gaussian formula in (2) as $f(x,y)$, obtained the formula of LoG as described in (3) where x and y are positions calculated from the center [9].

$$LoG(x,y) = -\frac{1}{\pi\sigma^4}\left[1 - \frac{x^2+y^2}{2\sigma^2}\right] e^{-\frac{x^2+y^2}{2\sigma^2}} \qquad (3)$$

This feature extraction is used to assign boundaries between segments. This feature extraction is only used for bottom ROI. The selected area is the trabecular bone segment that is the uppermost segment. The first step is to read the pre-processing image. The second step gets the image of Laplacian of Gaussian result. The third step is to get the top edge cortical bone. The fourth step is to fill the segment above the edge.

D. Segmentation

After getting the feature vector on each feature extraction, proceed to the classification process using Extreme Learning Machine. Extreme Learning Machine (ELM) proposed by Huang Et al. is one of the simplest feed-forward neural networks using a hidden node layer, where the weight of the hidden input is randomly selected and does not need to be adjusted, and the weight of the hidden-out is obtained by least squares regression or ridge regression. Since this model only studies the weight of hidden-output, the training process becomes faster [10].

The original ELM for binary classification with n hidden nodesfirst maps the p-dimensional input $\boldsymbol{x}$ into feature vector $h(x) = [1, h_1(x), h_2(x), \ldots, h_n(x)]^T$ with $(n+1)$ dimension, where $h_j(\boldsymbol{x})$ is represented in (4) and then approximates the class label $y \in \{-1, 1\}$ by linear combination of the components of feature vectors $h_j(\boldsymbol{x})$ denoted on (5).

$$h_j(x) = g\left(\sum_{k=1}^{p} a_{jk} X_k + b_j\right) = g(a_j^T x + b_j), j \in [1,n] \qquad (4)$$

$$\tilde{y} = \sum_{k=1}^{N} \beta_k h_k(\boldsymbol{x}) + \beta_0 = \boldsymbol{h}(\boldsymbol{x})^T \beta \qquad (5)$$

where $\alpha_j \in R^p$ and $b_j \in R$ are the parameter used in *jth*-hidden nodes which are random initialized and $\beta = [\beta_0, \beta_1, \ldots, \beta_n]^T \in R^{n+1}$ is weight of hidden-out, $g(\cdot)$ is sigmoid activation function. Weight of hidden-out β can be learned using linear regression or ridge regression.

In this research, 22184 pixel intensities were taken from eight ROI images. Those pixel intensities are used as training data and the ground truth on eight ROI images are used as a class label. The ELM model is then used in the testing process (pixel classification) where one segmentation process grouped 16,384 data. Pixel grouping by using ELM produces two classes: white and black.

E. Postprocessing

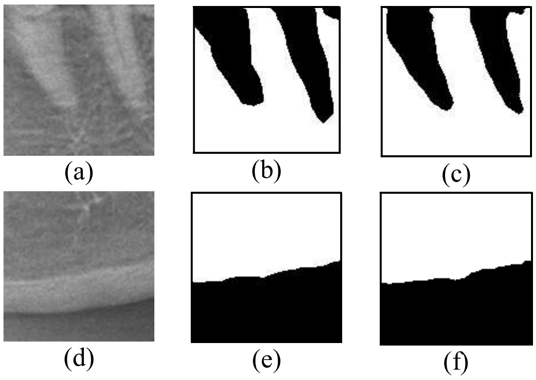

Fig. 6. Results of Segmentation (a) upper ROI image (b) upper ROI ground truth image (c) upper ROI segmentation result (d) lower ROI image (e) lower ROI ground truth image (f) lower ROI segmentation result

Postprocessing is a segmentation improvement on the segmented image. The first operation is to refine the segmentation results using the median filter. Then proceed with retrieving large area using matlab regionprops feature. This operation is done to clear the noise and fill the holes where the noise and hole have a small value area.

III. Experiment And Discussion

The data used is data that is processed using trabecular bone segmentation application. Data used as input is dental panoramic radiograph image of female patients with Asian race (Indonesia). From the dental panoramic radiograph image selected ROI is done manually by selecting four different square areas of two right and two left with a size of 128×128 pixels on the mandibular bone of the trabecular bone area containing the dental area for first ROI and cortical bone on the second ROI. The test used 20 input data. The output data from the trabecular bone segmentation is a black-and-white image with trabecular bone ROI. White color indicates trabecular bone and black color indicates non-trabecular bone.

At this experimental stage, each classification pixel is compared with each pixel in the ground truth data. Performance tests are applied to the upper ROI and lower ROI using the Extreme Learning Machine classification method in the segmentation process. This performance test calculates the accuracy, sensitivity, and specificity.

The testing process used 20 input data. The average of sensitivity, specificity, and accuracy on upper trabecular ROI are 82.31%, 93.67%, and 90.33%, respectively. While the average of sensitivity, specificity, and accuracy on lower trabecular ROI are 95.01%, 96.50%, and 95.29%, respectively as shown in **Error! Reference source not found.**I. The segmentation result of our proposed method are presented in Fig. 6.

IV. Conclusion

The purpose of this research is success to obtain the result of segmentation of trabecular bone structure on dental panoramic radiograph based on segment profile characteristics using Extreme Learning Machine method. In the upper ROI, the average of sensitivity, specificity, and accuracy were 82.31%, 93.67%, and 90.33%, respectively. In the lower ROI, the average of sensitivity, specificity, and accuracy were 95.01%, 96.50%, and 95.29%, respectively.

TABLE I. PERFORMANCE OF SEGMENTATION RESULTS

	Sensitivity	Specificity	Accuracy
Upper ROI	82.31 %	93.67 %	90.33 %
Lower ROI	95.01 %	96.50 %	95.29 %

Acknowledgment

The authors wish to acknowledge Ministry of Research, Technology and Higher Education of the Republic of Indonesia and Lembaga Penelitian dan Pengabdian kepada Masyarakat (LPPM) ITS, which have financed the program through the letter of agreement implementation research: 679/PKS/ITS/2017. Date: April 20th, 2017.

References

[1] A.Z. Arifin, A. Asano, A. Taguchi, T. Nakamoto, M. Ohtsuka, and K. Tanimoto, "Computer-aided system for measuring the mandibular cortical width on dental panoramic radiographs in identifying postmenopausal women with low bone mineral density," Osteoporosis International, vol. 17, no. 5, pp. 753-759, May 2006.

[2] A. Z. Arifin, D. I. M., I. Cholissodin, I. Lukmana, "Enhancement of Trabecular Bone on Dental Panoramic Radiographs Using Multiscale Line Operator," ICACSIS, pp. 343-346, 2011.

[3] L. R. Dewi, A. Z. Arifin, A. Yuniarty, "Segmentasi Trabecular Bone Berdasarkan Linear Structure pada Citra Dental Panoramic Radiographs," pp. 1-5, 2009.

[4] N. Yuniarti, A. Z. Arifin, M. Aryuni, "Informasi Tekstural untuk Identifikasi Trabecular Bone pada Citra Dental Panoramic Radiograph," pp. 1-5, 2008.

[5] C. Zhu, B. Zou, R. Zhao, J. Cui, X. Duanb, Z. Chen, Y. Liang, "Retinal vessel segmentation in colour fundus images using Extreme Learning Machine," Computerized Medical Imaging and Graphics, 2016.

[6] T. Lindeberg, "Edge detection and ridge detection with automatic scale," Int. J. Comput. Vis, no. 30, p. 117–156, 1998..

[7] D. J. Field, "Relations between the statistics of natural images and the response properties of cortical cells," J. Opt. Soc. Am. A, vol. 4, no. 12, pp. 2379-2394, 1987.

[8] P. Kovesi, "Image features from phase congruency," Computer Vision, pp. 1-26, 1995.

[9] R. Wang, "Laplacian of Gaussian (LoG)," 16 10 2016. [Online]. Available: http://fourier.eng.hmc.edu/e161/lectures/gradient/node8.html. [Accessed 1 19 2017].

Huang, G., Huang, G.B., Song, S., You, K. , "Trends in extreme learning machines: A review," Neural Networks, vol. 61, pp. 32-48, 2015.